Fragmentation of Shells

F. Wittel,[1] F. Kun,[2,*] H. J. Herrmann,[3] and B. H. Kröplin[1]

[1]*Institute of Statics and Dynamics of Aerospace Structures, University of Stuttgart, Pfaffenwaldring 27, 70569 Stuttgart, Germany*
[2]*Department of Theoretical Physics, University of Debrecen, P.O. Box:5, H-4010 Debrecen, Hungary*
[3]*ICA 1, University of Stuttgart, Pfaffenwaldring 27, D-70569 Stuttgart, Germany*

(Received 17 February 2004; published 16 July 2004)

We present a theoretical and experimental study of the fragmentation of closed thin shells made of a disordered brittle material. Experiments were performed on brown and white hen egg shells under two different loading conditions: impact with a hard wall and explosion by a combustible mixture. Both give rise to power law fragment size distributions. A three-dimensional discrete element model of shells is worked out. Based on simulations of the model, we give evidence that power law fragment mass distributions arise due to an underlying phase transition which proved to be abrupt for explosion and continuous for impact. We demonstrate that the fragmentation of closed shells defines a new universality class of fragmentation phenomena.

DOI: 10.1103/PhysRevLett.93.035504 PACS numbers: 62.20.Mk, 46.50.+a, 64.60.–i

Closed shells made of solid materials are often used in every day life and in industrial applications in the form of containers, pressure vessels, or combustion chambers. From a structural point of view, aircraft vehicles, launch vehicles such as rockets and building blocks of a space station, are also shell-like systems and even certain types of modern buildings can be considered as shells. The egg shell as nature's oldest container proved to be a reliable construction for protecting life. In many of the applications shell-like constructions operate under an internal pressure, and they usually fail due to an excess internal load which can arise either as a result of slowly driving the system above its stability limit or by a pressure pulse caused by an explosive shock inside the shell. Because of the widespread applications, the failure of shell systems is a very important scientific and technological problem which can also have an enormous social impact due to the human costs arising, for instance, from accidents.

Fragmentation, i.e., the breaking of particulate materials into smaller pieces, is abundant in nature, occurring on a broad range of length scales from meteor impacts through geological phenomena and industrial applications down to the breakup of large molecules and heavy nuclei [1–6]. The most striking observation concerning fragmentation is that the distribution of fragment sizes shows a power law behavior independent on the way of imparting energy, relevant microscopic interactions, and length scales involved, with an exponent depending only on the dimensionality of the system [2–10]. Detailed experimental and theoretical studies revealed that universality prevails for large enough input energies when the system falls apart into small enough pieces [2–6]; however, at lower energies, a systematic dependence of the exponent on the input energy is evident [10]. Recent investigations on the low energy limit of fragmentation suggest that the power law distribution of fragment sizes arises due to an underlying critical point [6–9]. Former studies on fragmentation have been focused on bulk systems in one, two, and three dimensions; however, hardly any studies have been devoted to the fragmentation of shells. The peculiarity of the fragmentation of closed shells originates from the fact that their local structure is inherently two-dimensional; however, the dynamics of the systems, the motion of material elements, deformation, and stress states are three-dimensional, which allows for a rich variety of failure modes.

In this Letter, we present a theoretical and experimental study of the fragmentation of closed brittle shells arising due to an excess load inside the shell. We performed experiments on the explosion and impact fragmentation of hen egg shells resulting in power law fragment size distributions. Based on large scale molecular dynamics simulations of a discrete element model of shells, we give evidence that power law fragment mass distributions arise due to an underlying phase transition which proved to be abrupt for explosion and continuous for impact. It is shown that the fragmentation of closed shells belongs to a universality class different from that of the two- and three-dimensional bulk systems. Our results also have important implications for the fragmentation of bulk systems.

For simplicity, our experiments were performed on ordinary brown and white egg shells, which consist of a natural disordered material with a high degree of brittleness. In the preparation, first two holes of regular circular shape were drilled in the bottom and in the top of the egg, through which the content of the egg was blown out. The inside was carefully washed and rinsed out several times, and finally the empty shells were dried in a microwave oven to get rid of all the moisture of the egg shell.

In the impact experiments, intact egg shells are catapulted against the ground at a high speed using a simple setup of rubber bands. In explosion experiments, initially the egg shell is flooded with hydrogen and hung vertically

inside a plastic bag. The combustion reaction is initiated by igniting the escaping hydrogen on the top of the egg. Because of the escaping hydrogen, oxygen is drawn up into the egg through the bottom hole. When enough air has entered to form a combustible mixture inside the egg, the flame penetrates through the top hole and the egg explodes. Both kinds of experiments were carried out inside a soft plastic bag so that secondary fragmentation due to the impact of fragments did not occur.

The resulting egg shell pieces are then carefully collected and placed on the tray of a scanner without overlap. In the scanned image, fragments appear as black spots on a white background, which were further analyzed by a cluster searching code. The mass of fragments was determined as the number of pixels of spots in the scanned image.

Three consecutive snapshots of the explosion process of an egg shell taken by a high speed camera of 400 Hz are presented in Fig. 1. Based on the snapshots the total duration of an explosion is estimated to be of the order of 1 msec. An example of scanned egg shell pieces can be seen in the inset of Fig. 2. Since the pressure which builds up during combustion can be slightly controlled by the hole size, i.e., the smaller the hole is, the higher the pressure at the explosion is, we performed several series of explosion experiments with hole diameters d between 1.2 and 2.5 mm. Figure 2 presents the fragment mass distributions $F(m)$ for impact and explosion experiments averaged over 10–20 egg shells for each curve. For the impact experiment, a power law behavior of the fragment mass distribution $F(m) \sim m^{-\tau}$ can be observed over 3 orders of magnitude where the value of the exponent can be determined with high precision to $\tau = 1.35 \pm 0.02$. Explosion experiments result also in a power law distribution of the same value of τ for small fragments with a relatively broad cutoff for the large ones. Smaller hole diameter d in Fig. 2, i.e., higher pressure, gives rise to a larger number of fragments with a smaller cutoff mass and a faster decay of the distribution $F(m)$ at the large fragments. Comparing the number of fragments obtained, the ratio of the pressure values in the explosions at hole diameters $d = 1.2$ and 2.0 mm, presented in Fig. 2, was estimated to be about 1.6. Note that the relatively small value of the exponent τ can indicate a cleavage mechanism of shell fragmentation and is significantly different from the experimental and theoretical results on fragmenting two-dimensional bulk systems where $1.5 \leq \tau \leq 2$ has been found and from the three-dimensional ones where $\tau > 2$ is obtained [2–10].

Our theoretical study is restricted for simplicity to spherical shells; i.e., we worked out a three-dimensional discrete element model of spherical shells by discretizing the surface of the unit sphere into randomly shaped triangles (Delaunay triangulation). The nodes of the triangulation represent pointlike material elements in the model whose masses are defined by the area of the dual Voronoi polygon [11] assigned to it. The bonds between nodes are assumed to be springs having linear elastic behavior up to failure. Disorder is introduced in the model solely by the randomness of the tessellation so that the masses of the nodes and the lengths and the cross sections of the springs are determined by the tessellation (quenched structural disorder). After prescribing the initial conditions of a specific fragmentation process studied, the time evolution of the system is followed by solving the equation of motion of the nodes. In order to account for crack formation in the model, springs are assumed to break during the time evolution of the system when their deformation ε exceeds a fixed breaking threshold ε_c, resulting in a random sequence of breakings due to the disordered spring properties. As a result of successive spring breakings, cracks nucleate, grow, and merge on the spherical surface, giving rise to the complete breakup of the shell into pieces. Fragments of the shell are defined in the model as sets of nodes connected by the remaining intact springs. The process is stopped when the system has attained a relaxed state.

In the computer simulations two different ways of loading have been considered, which model the experimental conditions and represent limiting cases of energy input rates: (i) *pressure pulse* and (ii) *impact* load starting from an initially stress-free state. A pressure pulse in a

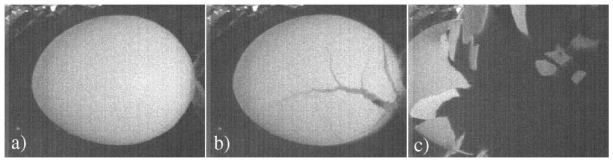

FIG. 1. Time evolution of the explosion of an egg shell. (a) Ignition, (b) instant of explosion, (c) final state.

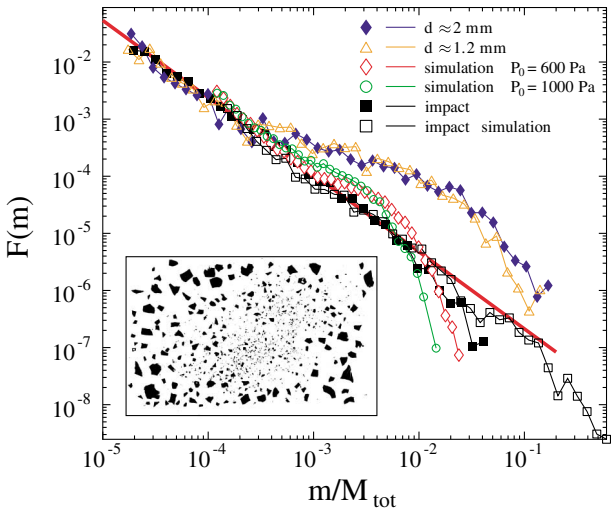

FIG. 2 (color online). Comparison of fragment mass distributions obtained in explosion experiments with two hole sizes and in the impact experiment to the simulation results. Inset: scanned pieces of an impact experiment.

shell is carried out by imposing a fixed internal pressure P_0, from which the forces acting on the material elements are calculated. The constant pressure P_0 gives rise to an expansion of the system with a continuous increase of the imparted energy $E_{\text{tot}} = P_0 \Delta V$, where ΔV denotes the volume change with respect to the initial volume V_0. Since the force F acting on the shell is proportional to the actual surface area A, the system is driven by an increasing force $F \sim P_0 A$ during the expansion process; see Fig. 3(b). The impact loading realizes the limiting case of instantaneous energy input $E_{\text{tot}} = E_0$ by giving a fixed initial radially oriented velocity v_0 to all material elements; see Fig. 3(a). Simulations performed varying the control parameters P_0 and E_0 in a broad range revealed that for both loading cases there exists a critical value P_c and E_c, below which the shell keeps its integrity, suffering only partial failure in the form of cracks (damaged state); above it, however, complete breakup occurs into pieces (fragmented state). Since the breakup of the shell under pressure (impact) loading is analogous to the stress (strain) controlled fracture of disordered bulk solids, the transitions between the damaged and fragmented states arises abruptly (continuously) at the critical point.

Quantitative characterization of the breakup process when increasing the control parameter can be given by monitoring the average mass of the largest fragment normalized by the total mass $\langle M_{\text{max}}/M_{\text{tot}} \rangle$. M_{max} is a monotonically decreasing function of both P_0 and E_0. However, the functional forms are different in the two cases; see Fig. 4. At low pressure values in Fig. 4, M_{max} is practically equal to the total mass since hardly any fragments are formed. Above P_c, however, M_{max} gets significantly smaller than M_{tot}, indicating the disintegration of the shell into pieces. The value of the critical pressure P_c needed to achieve fragmentation and the functional form of the curve above P_c were determined by plotting $\langle M_{\text{max}}/M_{\text{tot}} \rangle$ as a function of the difference $|P_0 - P_c|$, varying P_c until a straight line is obtained in a double logarithmic plot. The power law dependence on the distance from the critical point $\langle M_{\text{max}}/M_{\text{tot}} \rangle \sim |P_0 - P_c|^{-\alpha}$ for $P_0 > P_c$ is evidenced by Fig. 5(a), where $\alpha = 0.66 \pm 0.02$ was determined. The finite jump of M_{max} at P in Fig. 4 indicates the abrupt nature of the transition between the two regimes. For impact loading, $\langle M_{\text{max}}/M_{\text{tot}} \rangle$ proved to be a continuous function of E_0; however, it also shows the existence of two regimes with a transition at a critical energy E_c. In Fig. 5(a) we show $\langle M_{\text{max}}/M_{\text{tot}} \rangle$ as a function of the distance from the critical point $|E_0 - E_c|$, where E_c was determined numerically in the same way as P_c. As opposed to the pressure loading, $\langle M_{\text{max}}/M_{\text{tot}} \rangle$ exhibits a power law behavior on both sides of the critical point but with different exponents $\langle M_{\text{max}}/M_{\text{tot}} \rangle \sim |E_0 - E_c|^{\beta}$ for $E_0 < E_c$ and $\langle M_{\text{max}}/M_{\text{tot}} \rangle \sim |E_0 - E_c|^{-\alpha}$ for $E_0 > E_c$, where the exponents were obtained as $\beta = 0.5 \pm 0.02$ and $\alpha = 0.66 \pm 0.02$. Note that in Fig. 5(a) for explosion only those data points of Fig. 4 are included which are above the critical point $P_0 > P_c$, and hence, the corresponding curve has only one decreasing branch. However, in the case of impact, data points on both sides of the critical point are presented so that the corresponding curve has two branches. The increasing branch belongs to the regime below the critical energy $E_0 < E_c$ characterized by the exponent β, while the decreasing branch is determined by data points above the critical energy $E_0 > E_c$ characterized by the exponent α. The value of α coincides in the two loading cases.

We also evaluated the mass-weighted average fragment mass $\overline{M}$ as the average value of the ratio of the second M_2 and first M_1 moments of the fragment mass distribution, subtracting the mass of the largest fragment from the sum [7]. The behavior of $\overline{M}$ shows clearly again the existence of two regimes of the breakup process with a transition at the critical point P_c and E_c. Under pressure loading, due to the abrupt disintegration $\overline{M}$ can be evaluated only above the critical point P_c, while for the impact case $\overline{M}$ has a maximum at the critical energy E_c typical for continuous phase transitions. Figure 5(b) demonstrates that in both loading cases $\overline{M}$ has a power law dependence

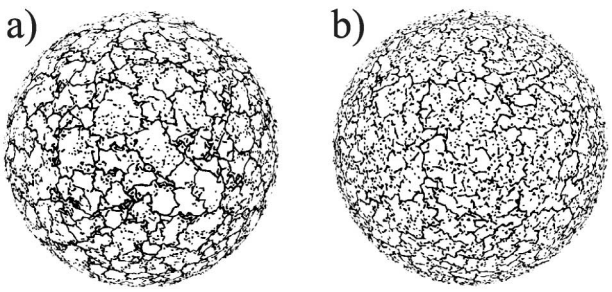

FIG. 3. Final fragmented states for (a) impact and (b) pressure pulse loading. Particle positions are projected back to the initial state on the surface. Black lines indicate cracks.

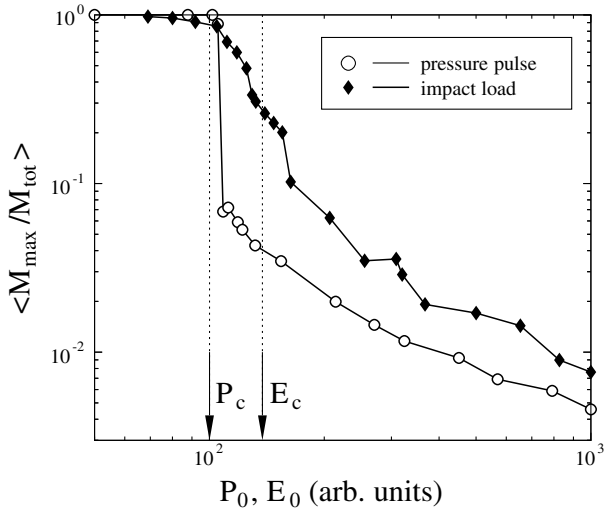

FIG. 4. $\langle M_{\text{max}}/M_{\text{tot}} \rangle$ versus P_0 and E_0. The values of P_c and E_c are also indicated.

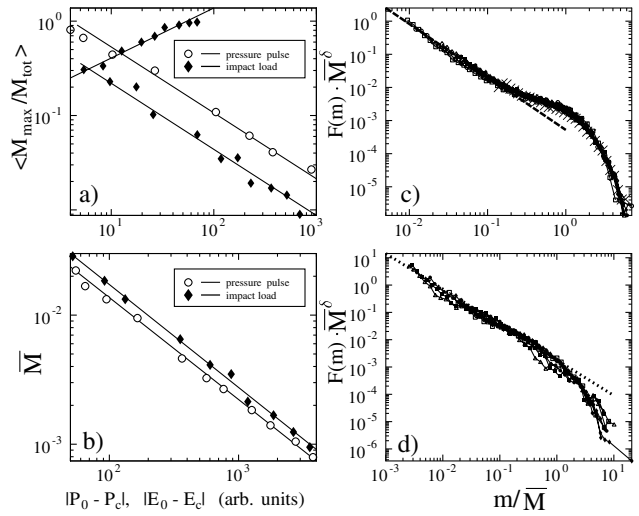

FIG. 5. Normalized mass of the largest fragment (a) and average fragment mass (b) as a function of the distance from the critical point. Rescaled plots of the fragment mass distributions (c) for explosion and (d) for impact.

on the distance from the critical point; i.e., $\overline{M} \sim |E_0 - E_c|^{-\gamma}$, and $\overline{M} \sim |P_0 - P_c|^{-\gamma}$ with the same value of the exponent $\gamma = 0.8 \pm 0.02$.

The most important characteristic quantity of our system, which can also be compared to the experimental results, is the mass distribution of fragments $F(m)$. For pressure loading, $F(m)$ can only be evaluated above P_c. Under impact loading for $E_0 < E_c$ we found that $F(m)$ has a pronounced peak at large fragments, indicating the presence of large damaged pieces. Approaching the critical point E_c, the peak gradually disappears and the distribution asymptotically becomes a power law at E_c. Above the critical point the power law remains for small fragments, followed by an exponential cutoff for the large ones. For the purpose of comparison, a mass distribution $F(m)$ obtained at an impact energy close to the critical point E_c and distributions at two different pressure values P_0 of the ratio 1.6 are plotted in Fig. 2 along with the experimental results. For impact an excellent agreement of the experimental and theoretical results is evidenced. For pressure loading, the functional form of $F(m)$ has a nice qualitative agreement with the experimental findings on the explosion of eggs. Furthermore, distributions at the same ratio of pressure values obtained by simulations and experiments proved to show the same tendency of evolution; see Fig. 2. Figures 5(c) and 5(d) demonstrate that by rescaling the mass distributions above the critical point by plotting $F(m)\overline{M}^{\delta}$ as a function of $m/\overline{M}$ an excellent data collapse is obtained with $\delta = 1.6 \pm 0.03$. The data collapse implies the validity of the scaling form $F(m) \sim m^{-\tau} f(m/\overline{M})$, typical for critical phenomena. The cutoff function f has a simple exponential form $\exp(-m/\overline{M})$ for impact loading, and a more complex one containing also an exponential component for the pressure case. The rescaled plots make possible an accurate determination of the exponent τ, where $\tau = 1.35 \pm 0.03$ and $\tau = 1.55 \pm 0.03$ were obtained for impact and pressure loading, respectively. Hence, a good quantitative agreement of the theoretical and experimental values of the exponent τ is evidenced for the impact loading of shells; however, for the case of pressure loading, the numerically obtained exponent turned out to be higher than in the case of exploded eggs.

In the fragmentation of bulk systems under appropriate conditions, a so-called detachment effect is observed when a surface layer breaks off from the bulk and undergoes a separated fragmentation process [7,10]. This effect also shows up in the fragment mass distributions in the form of a power law regime of small fragments of an exponent smaller than for the large ones. Our results on shell fragmentation can also provide a possible explanation of this kind of composite power laws of bulk fragmentation [7,10] and might even be relevant for the study of mass redistribution following super nova explosions in the Universe.

This work was supported by Projects No. SFB381 and No. OTKA T037212, M041537. F. K. was supported by the FKFP 0118/2001 and by the Gy. Békési Foundation of HAS.

*Electronic address: feri@dtp.atomki.hu

[1] J. J. Gilvarry, J. Appl. Phys. **32**, 391 (1961); J. Appl. Phys. **32**, 400 (1961).
[2] D. L. Turcotte, J. Geophys. Res. **91**, 1921 (1986).
[3] L. Oddershede, P. Dimon, and J. Bohr, Phys. Rev. Lett. **71**, 3107 (1993); A. Meibom and I. Balslev, Phys. Rev. Lett. **76**, 2492 (1996).
[4] T. Kadono and M. Arakawa, Phys. Rev. E **65**, 035107 (2002); T. Kadono, Phys. Rev. Lett. **78**, 1444 (1997).
[5] H. Inaoka, E. Toyosawa, and H. Takayasu, Phys. Rev. Lett. **78**, 3455 (1997); H. Inaoka and H. Takayasu, Physica (Amsterdam) **229A**, 1 (1996).
[6] H. Katsuragi, D. Sugino, and H. Honjo, Phys. Rev. E **68**, 046105 (2003).
[7] F. Kun and H. J. Herrmann, Phys. Rev. E **59**, 2623 (1999); Comp. Meth. Appl. Mech. Eng. **138**, 3 (1996); Int. J. Mod. Phys. C **7**, 837 (1996).
[8] J. Åström and J. Timonen, Phys. Rev. Lett. **78**, 3677 (1997); J. Åström, M. Kellomäki, and J. Timonen, Phys. Rev. E **55**, 4757 (1997).
[9] J. A. Aström, B. L. Holian, and J. Timonen, Phys. Rev. Lett. **84**, 3061 (2000); W. T. Ashurst and B. L. Holian, Phys. Rev. E **59**, 6742 (1999).
[10] E. S. C. Ching, S. Liu, and K.-Q. Xia, Physica (Amsterdam) **287A**, 83 (2000); A. Bershadskii, J. Phys. A **33**, 2179 (2000); A. Diehl *et al.*, Phys. Rev. E **62**, 4742 (2000).
[11] K. B. Lauritsen, H. Puhl, and H. J. Tillemans, Int. J. Mod. Phys. C **5**, 909 (1994).